ISBN: 978-3-95450-261-5 ISSN: 2673-7000 doi: 10.18429/JACoW-NAPAC2025-WEP067

STUDY OF UNCORRELATED RESONANCE CROSSING IN A CONTROLLED ENVIRONMENT

Jack Kelley*,[1,2], Oleksii Beznosov,[1], Joseph Devlin,[3], D. P. Barber,[4]
[1]Los Alamos National Laboratory, Los Alamos, NM, USA
[2]Virginia Tech, Blacksburg, VA, USA [3]Cornell University, Ithaca, IL, USA
[4]University of New Mexico, Albuquerque, NM, USA

Abstract

This paper deals with estimating spin depolarization in planned very high energy electron-positron storage rings like the FCC-ee. The paper covers three aspects of the work: 1) the putative so-called uncorrelated resonance crossing due to noise in the spin-rotation phase advance caused by photon emission in synchrotron radiation. This is expected to suppress the depolarization caused by synchrotron sideband resonances, 2) a study of the performance of our code on multiple high performance systems, and 3) the novel exploitation of a high order Magnus expansion applied to spin transport. The study uses Monte-Carlo spin-orbit tracking for a simple model of spin motion, the so-called single resonance model, augmented by the effects of radiation. The results presented here represent the first steps of a planned detailed large-scale exploration.

INTRODUCTION

We make use of a simple one-degree of freedom model (hereafter referred to as SM1) for an electron storage ring, first discussed in Ref. [1]. SM1 is adapted from the so-called single resonance model (SRM) [2] by adding a noise term and damping to model depolarization of electrons due to spin diffusion in the trivial setting of the SRM. In SM1, a particle with normalized phase-space coordinates is modeled as a 2D random process $Y(\theta) = (Y_1(\theta), Y_2(\theta))$ governed by the stochastic differential equation (SDE)

$$\mathrm{d}Y = (-bJY - \varepsilon Y)\mathrm{d}\theta + \sqrt{\varepsilon}\mathrm{d}W_\theta,\ J = \begin{bmatrix} 0 & 1 \\ -1 & 0 \end{bmatrix}, \quad (1)$$

with the initial values of Y belonging to the distribution $Y(0) \sim \mathcal{N}_2(0, \frac{1}{2}I_2)$ where I_2 is the 2×2 identity matrix. Here W_θ denotes the two-dimensional Wiener process, and b and ε are constant parameters that model the betatron oscillation frequency and the synchrotron radiation strength, respectively.

Note that if $\varepsilon = 0$, that is, noise and damping are not present, the model reduces to a simple harmonic oscillator with frequency b. Further note that if noise is ignored, we get a deterministic, damped harmonic oscillator with random initial condition with a known solution for every random sample. This makes this problem amenable to the exponential Euler method, where each step is a result of evaluating

$$Y(\theta_{n+1}) = e^{-\Delta\theta(bJ+\varepsilon I)}Y(\theta_n) + \sqrt{\varepsilon}\Delta W_n, \quad (2)$$

where the components of the two-vector ΔW_n are sampled from the normal distribution $\mathcal{N}(0, \sqrt{h})$ independently at each step for a step size $h = \Delta\theta$. Note that, since the Stern-Gerlach effect can be neglected at high energy, the orbital equations can be solved independently of the spin equation, but the spin equation requires intermediate samples at azimuths θ_n.

THOMAS-BMT EQUATION FOR SM1

The matrix version of the spin equation for SM1 is

$$\frac{\mathrm{d}S}{\mathrm{d}\theta} = \Omega(Y(\theta))S,\ \ \Omega(Y) = \nu_0 J_0 + \sigma_0 \sum_{j=1}^{2} J_j Y_j, \quad (3)$$

where $\vec{S}$ is the unit-norm spin vector with initial condition $\vec{S}(0) = \vec{S}_0$ and $J_0^{1,2} = J_1^{3,2} = J_2^{1,3} = 1$.

Here ν_0, the spin tune on the closed design orbit, models spin precession frequency around the vertical, and σ_0 is the so-called resonance strength. In the absence of damping and diffusion, the invariant spin field (ISF) in our model is given by

$$\hat{n}(y) = \frac{1}{\sigma(y)}\begin{pmatrix} y_1 \\ y_2 \\ \zeta \end{pmatrix},\ \ \sigma(y) := \sqrt{y^{\mathrm{T}}y + \zeta^2},\ \ \zeta := \frac{\nu_0 - b}{\sigma_0}. \quad (4)$$

Then, as a first step to going beyond SM1 and modeling noise in the spin phase advance, we add a modulation at the synchrotron tune and add noise to that tune. Then ν_0 is replaced by

$$\nu = \nu_0(1 + \delta\sin((\nu_s + \xi)\theta + \phi)) \quad (5)$$

where ν_s in the synchrotron tune. We choose a typical fractional energy spread $\delta = 0.005$ and a typical ν_s of 0.03 while $\xi \sim \mathcal{N}(0, 0.001)$. δ is proportional to $\frac{\Delta E}{E}$.

NUMERICAL METHOD

While in the previous section we have described our spin with a 3-vector, in our numerical method we compute the spin update via an accumulated quaternion q before transforming q back to a matrix in $\mathbb{R}^{3\times3}$ to take measurements. To compute the procession of each particle's spin through the ring we keep track of q, which represents the rotation of the spin vector S from its initial position S_0 to the current position $S(\theta)$. We start the simulation with q_0 corresponding to the quaternion $\langle 1, 0, 0, 0\rangle$ and update this rotation quaternion

* jackkelley@vt.edu

ISBN: 978-3-95450-261-5 ISSN: 2673-7000 doi: 10.18429/JACoW-NAPAC2025-WEP067

at each step. For q_θ at some step θ, we update the rotation by solving for a spin update quaternion q_S, then we compute

$$q_{\theta+1} = q_S \circ q_\theta \tag{6}$$

where $A \circ B$ denotes the Hamilton product of A and B. To update a particle's spin unit 3-vector S to take a measurement, we transform q into a 3x3 rotation map and multiply that map with S_0.

We will now discuss how we compute the step update q_S. Since q is a unit quaternion belonging to Lie group SU(2), any update to it that is a rotation must result in another unit quaternion, thus q_S belongs to SU(2). Therefore we can write the exact solution as $\exp(X(h))$ where $X(h)$ must be in SU(2) [3]:

$$q_{\theta+1} = \exp(X(h))q_\theta \tag{7}$$

Knowing this, we can find a power expansion of $X(h)$ using the Magnus expansion, which has the useful property that at every order the Magnus expansion of $X(h)$ belongs to SU(2) and therefore $\exp(X(h))$ describes a rotation, even when the power series is truncated. This property also means that we never need to re-normalize our rotation quaternion throughout the integration.

For the implementation of our Magnus integrator, we follow Ref. [4] and use a 6th order expansion, requiring the computation of three sets of phase space coordinates for each time step. For some step size h, we solve for the exact orbital coordinates with Eq. (2) with the noise excluded.

The orbital dynamics are evaluated at three Gauss-Legendre quadrature nodes

$$\theta_1 = \theta + \left(\frac{1}{2} - \frac{\sqrt{15}}{10}\right)h,$$
$$\theta_2 = \theta + \frac{1}{2}h,$$
$$\theta_3 = \theta + \left(\frac{1}{2} + \frac{\sqrt{15}}{10}\right)h.$$

First we define

$$A_i = \frac{-i}{2}\beta_i(\theta)\cdot\vec{\sigma},\ \beta_i = \begin{bmatrix}\sigma_0 Y_1(\theta_i)\\ \sigma_0 Y_2(\theta_i)\\ \nu_0\end{bmatrix},\ i = 1,2,3, \tag{8}$$

one for each of the three nodes, where $\vec{\sigma}$ is the vector of Pauli matrices. Then we solve for X, which for 6th order is defined as follows:

$$X = \alpha_1 + \frac{1}{12}\alpha_3 + \frac{1}{240}[-20\alpha_1 - \alpha_3 + C_1, \alpha_2 + C_2],$$

$$\alpha_1 = hA_2,\ \alpha_2 = \frac{\sqrt{15}h}{3}(A_3 - A_1),\ \alpha_3 = \frac{10h}{3}(A_3 - 2A_2 + A_1)$$

$$C_1 = [\alpha_1, \alpha_2],\ C_2 = -\frac{1}{60}[\alpha_1, 2\alpha_3 + C_1]$$

where $[F, G] = FG - GF$.

With everything included, X becomes

$$X = \begin{bmatrix}\frac{1}{2}h\nu_0\\ -\frac{5}{18}h\sigma_0 Y_2(\theta_1) - \frac{4}{9}h\sigma_0 Y_2(\theta_2) - \frac{5}{18}h\sigma_0 Y_2(\theta_3)\\ -\frac{5}{18}h\sigma_0 Y_1(\theta_1) - \frac{4}{9}h\sigma_0 Y_1(\theta_2) - \frac{5}{18}h\sigma_0 Y_1(\theta_3)\end{bmatrix}.$$

This vector is exponentiated into a quaternion via the following set of formulas

$$\|X\| = \sqrt{X_1^2 + X_2^2 + X_3^2}$$

$$q_{new} = \begin{bmatrix}-\cos(\|X\|)\\ \mathrm{sinc}(\|X\|)X_1\\ \mathrm{sinc}(\|X\|)X_2\\ \mathrm{sinc}(\|X\|)X_3\end{bmatrix}, \tag{9}$$

which is in turn used in Eq. (6) to update the rotation quaternion.

One major advantage of this scheme is that we are able to take relatively large steps in theta, drastically reducing the computational cost.

RESULTS

Our results demonstrate that our spin-tracking code is able to closely match the ISF approximation described in Ref. [1] and also be adapted to study more complex phenomena. We have chosen the parameters of the HERA ring [5] for our simulations, both to provide realistic parameters and to allow us to compare our findings with previous results.

We are interested in the equilibrium polarization P_{eq} of the particles, which is the result of the balance between the Sokolov-Ternov polarization and the depolarization rate within the ring. In the ISF approximation, particles are depolarized according to the depolarization time constant τ_{dep} as calculated in Ref. [1]. In our simulation, τ_{dep} is obtained via a non-linear least squares fit.

In Fig. 1 we see that our kinetic simulation closely matches the ISF approximation when noise is not included. When we introduce noise into b such that the final orbital update at each step has $b(\theta) = b + 4\xi$, $\xi \sim \mathcal{N}(0,1)$, we observe the equilibrium polarizations to spread out more over ν_0.

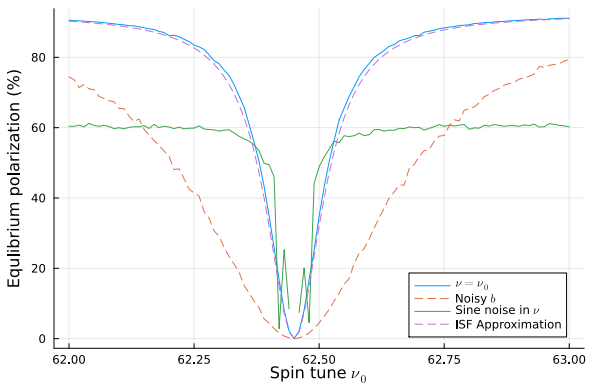

Figure 1: Spin tune scan for 4096 particles.

ISBN: 978-3-95450-261-5 ISSN: 2673-7000 doi: 10.18429/JACoW-NAPAC2025-WEP067

When we instead modulate ν according to $\nu(\theta) = \nu_0(1 + \delta \sin((0.03 + \xi)\theta))$, $\xi \sim \mathcal{N}(0, 0.001)$ and set $\varepsilon = 0$, we observe sideband resonances.

In Fig. 2 we see that the amplitude of the early oscillations (e.g. the transient behavior) in polarization are lower for the simulation in which particles were initialized with their spins along the ISF as opposed to along the vertical axis, while the frequency is the same. This follows our intuition, as we would expect the particles to have a tendency to align themselves with the ISF, so as their spins are closer to the ISF the amplitude of their oscillations will be lower.

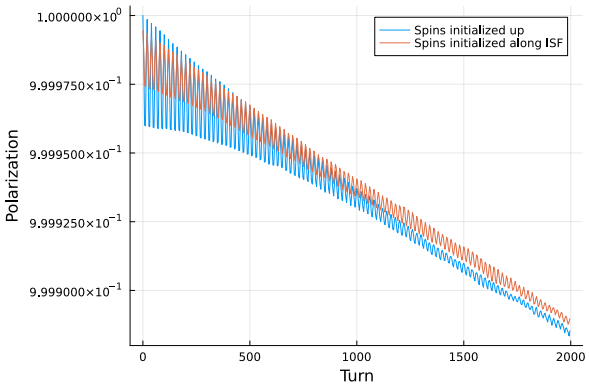

Figure 2: Polarization vs. turns for different initial spin alignments for 4096 particles.

COMPUTATIONAL PERFORMANCE

In this section, we wish to discuss the performance of our spin-tracking code on various hardware. The program was written in Julia and uses the CUDA.jl package, allowing us to write CUDA kernels that run on a GPU. The numerical method described above is run entirely on a GPU, allowing us to simulate tens of thousands of particles with little overhead.

In Fig. 3 we show a throughput roofline of our integration kernel for 1024, 2048, and 4096 particles run on an Nvidia A2000 desktop GPU. We note that as the number of particles increases, the performance as well as the arithmetic intensity increase, indicating that the code scales well with the number of particles as increasing the number of particles actually increases the ratio of computation to memory transfer.

We also profiled our code on a higher performance Nvidia A100 GPU, as shown in Fig. 4, for a larger number of particles than on the A2000. We observe the same scaling behavior as before.

All profiling tests, as shown in Tables 1 and 2, were run with a step size $h = 5 \times 10^{-4}$.

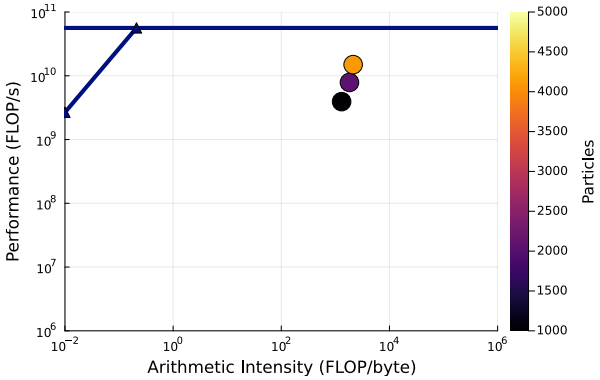

Figure 3: Nvidia A2000 throughput roofline.

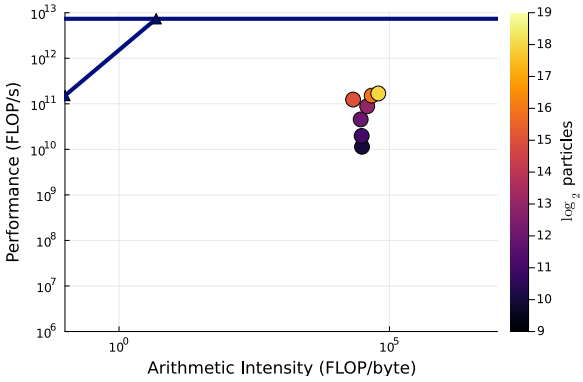

Figure 4: Nvidia A100 throughput roofline.

Table 1: Nvidia A2000 Profiling Results

Particle Count	FLOP/byte	FLOP/s	Turns
1024	1303.95	3.93×10^9	1
2048	1822.23	7.86×10^9	1
4096	2130.26	1.50×10^{10}	1

Table 2: Nvidia A100 Profiling Results

Particle Count	FLOP/byte	FLOP/s	Turns
1024	31074.11	1.14×10^{10}	10
2048	30656.78	1.97×10^{10}	10
4096	29357.33	4.55×10^{10}	10
8192	38789.18	8.84×10^{10}	10
32768	21267.12	1.24×10^{11}	10
65536	46962.47	1.51×10^{11}	10
262144	62095.75	1.69×10^{11}	10

ACKNOWLEDGEMENTS

We thank the U.S. Department of Energy (DOE), Office of Science, Accelerator R&D and Production (ARDAP) subprogram for support under award numbers DE-SC0025476 and DE-SC0025351, and at the Los Alamos National Laboratory (LANL) under DOE Contract No. 89233218CNA000001.

This research used resources of the National Energy Research Scientific Computing Center (NERSC), a DOE Office of Science User Facility, using NERSC award HEP-ERCAP0034811. We would also like to thank James Ellison and Klaus Heinemann for sharing their knowledge on the subject of spin dynamics and for their help in reviewing this paper.

ISBN: 978-3-95450-261-5 ISSN: 2673-7000 doi: 10.18429/JACoW-NAPAC2025-WEP067

REFERENCES

[1] O. Beznosov, "From wave propagation to spin dynamics: Mathematical and computational aspects", Ph.D. dissertation, University of New Mexico, 2020. https://www.proquest.com/dissertations-theses/wave-propagation-spin-dynamics-mathematical/docview/2512815190/se-2

[2] D. P. Barber, J. A. Ellison, and K. Heinemann, "Quasiperiodic spin-orbit motion and spin tunes in storage rings", *Phys. Rev. Spec. Top. Accel. Beams*, vol. 7, no. 12, p. 124 002, 2004. doi:10.1103/PhysRevSTAB.7.124002

[3] D. Sagan, "Bmad: A relativistic charged particle simulation library", *Nucl. Instrum. Methods Phys. Res. A*, vol. 558, no. 1, pp. 356–359, 2006. doi:10.1016/j.nima.2005.11.001

[4] S. Blanes, F. Casas, J. Oteo, and J. Ros, "The magnus expansion and some of its applications", *Phys. Rep.*, vol. 470, no. 5, pp. 151–238, 2009. doi:10.1016/j.physrep.2008.11.001

[5] D. P. Barber *et al.*, "The first achievement of longitudinal spin polarization in a high energy electron storage ring", *Phys. Lett. B*, vol. 343, no. 1, pp. 436–443, 1995. doi:10.1016/0370-2693(94)01465-O